



## Pectic polysaccharides from *Aconitum carmichaelii* leaves protects against DSS-induced ulcerative colitis in mice through modulations of metabolism and microbiota composition

Yu-Ping Fu<sup>a,\*</sup>, Cen-Yu Li<sup>b</sup>, Xi Peng<sup>b</sup>, Helle Wangensteen<sup>a</sup>, Kari Tvete Inngjerdigen<sup>a</sup>, Yuan-Feng Zou<sup>b,\*</sup>

<sup>a</sup> Section for Pharmaceutical Chemistry, Department of Pharmacy, University of Oslo, P.O. Box 1068 Blindern, 0316 Oslo, Norway

<sup>b</sup> Natural Medicine Research Center, College of Veterinary Medicine, Sichuan Agricultural University, 611130 Wenjiang, PR China

### ARTICLE INFO

#### Keywords:

*Aconitum carmichaelii* leaves  
Pectic polysaccharide  
Ulcerative colitis  
Metabolomics  
Gut microbiota

### ABSTRACT

The industrial processing of *Aconitum carmichaelii* roots for use in Traditional Chinese Medicine generates a high amount of waste material, especially leaves. An acidic polysaccharide fraction isolated from these unutilized leaves, AL-I, was in our previous work shown to contain pectic polysaccharides. This study aimed to investigate the protective effect of AL-I on ulcerative colitis for the possible application of *A. carmichaelii* leaves in the treatment of intestinal inflammatory diseases. AL-I was found to alleviate symptoms and colonic pathological injury in colitis mice, and ameliorate the levels of inflammatory indices in serum and colon. The production of short- and branched-chain fatty acids was also restored by AL-I. The observed protective effect could be due to the inhibition of NOD1 and TLR4 activation, the promotion of gene transcription of tight-junction proteins, and the modulation of gut microbiota composition like *Bacteroides*, *Dubosiella*, *Alistipes* and *Prevotella*. A regulation of serum metabolomic profiles being relevant to the bacterial change, such as D-mannose 6-phosphate, D-erythrose 4-phosphate and uric acid, was also observed.

### 1. Introduction

During the industrial production of Traditional Chinese medicine (TCM), a huge amount of unutilized plant parts are generated without further usage, such as stems and leaves for traditional medicines based on roots. These plant parts could be suitable plant resources for the production of phytochemicals [1]. The lateral (“FuZi”) and mother roots (“Chuanwu”) of *Aconitum carmichaelii* Debeaux (Ranunculaceae) are commonly used in TCM as analgesic and anesthetic agents, and to heal shock resulting from acute myocardial infarction and coronary heart disease [2,3]. After the roots of *A. carmichaelii* are harvested, the aerial parts are normally discarded, resulting in a vast amount of waste of this medicinal plant. To date, the aerial parts of *A. carmichaelii* have shown similar analgesic and anti-inflammatory activities as for the roots [4]. An acidic polysaccharide fraction composed of pectic polysaccharides isolated from *A. carmichaelii* leaves and structurally characterized in a previous study, was shown to possess immunomodulatory and intestinal anti-inflammatory activities in vitro [5].

Ulcerative colitis is a chronic intestinal inflammatory bowel disease,

and the number of cases worldwide has increased during the last decades. Inflammation of colonic epithelial cells and defects on mucous and epithelial barriers are factors strongly implicated in the pathogenesis of ulcerative colitis, in addition to microbiota dysbiosis [6]. The stability of gut microbiota is essential for human health and its interaction with the host determines the integrity of the intestinal mucosal barrier. In ulcerative colitis, the microbiota is characterized by reduced biodiversity, abnormal composition, and altered spatial distribution [7]. Further, certain classes of metabolites, deriving from bacterial metabolism of dietary substances or other molecules, have been implicated in the pathogenesis of intestinal bowel diseases [8].

There are mainly three types of classic drugs used for treating intestinal bowel disease at present, including aminosalicic acid derivatives, glucocorticoids, and immunosuppressants. However, due to the possible side effects after long-term of treatment, new treatment options are needed. Natural plant polysaccharides, as indigestible polymers, have low toxicity and have been shown to affect the intestinal immune system and restore barrier function in ulcerative colitis [9,10]. Pectins, for instance, have attracted growing attention in treatment or

\* Corresponding authors.

E-mail addresses: [y.p.fu@farmasi.uio.no](mailto:y.p.fu@farmasi.uio.no) (Y.-P. Fu), [yuanfengzou@sicau.edu.cn](mailto:yuanfengzou@sicau.edu.cn) (Y.-F. Zou).

<https://doi.org/10.1016/j.bioph.2022.113767>

Received 11 August 2022; Received in revised form 15 September 2022; Accepted 26 September 2022

Available online 4 October 2022

0753-3322/© 2022 The Author(s). Published by Elsevier Masson SAS. This is an open access article under the CC BY license (<http://creativecommons.org/licenses/by/4.0/>).

prevention of ulcerative colitis through regulation of intestinal microbiota composition, strengthening of intestinal barrier function, enhancement of antioxidant activities, promotion of short-fatty acids (SCFAs) production and reduction of pro-inflammatory mediators [9,11,12]. Therefore, based on the promising intestinal anti-inflammatory effects observed *in vitro*, we hypothesized that the pectic polysaccharides of *A. carmichaelii* leaves could alleviate dextran sulfate sodium (DSS)-induced ulcerative colitis in an *in vivo* mouse model.

This study aimed to broaden the utilization of *A. carmichaelii* leaves from the aspect of polysaccharides and to investigate the protective effects on DSS-induced ulcerative colitis. Metabolomic and microbiota analysis were performed to study the underlying mechanisms of the protective effect.

## 2. Materials and methods

### 2.1. Materials

The whole plant of *A. carmichaelii* Debeaux was collected from Jiangyou City, Sichuan Province, P.R. China in June 2019 (31°50'24.0"N/ 104°47'24.0"E, 517 m. a.s.l.). The fresh leaves were separated and processed as earlier reported [5].

### 2.2. Isolation, chemical composition and average-molecular weight of an acidic polysaccharide from *A. carmichaelii* leaves

A major acidic polysaccharide fraction, AL-I, was isolated from the water extract of dried leaves of *A. carmichaelii* by anion exchange chromatography, as earlier described [5]. The monosaccharide composition of AL-I was determined as trimethylsilylated (TMS) derivatives, after methanolysis by GC (Trace™ 1300 GC, Thermo Scientific™, Milan, Italy), as described by Chambers and Clamp [13] with modifications [14]. The total amounts of phenolic compounds and proteins of AL-I were determined by Folin-Ciocalteu [15] and Bio-Rad protein assay [16], respectively. The average-weight molecular weight (*Mw*) was determined by size exclusion chromatography and calculated by known dextran standards as previously described [5].

### 2.3. Protective effects of AL-I on ulcerative colitis mice

#### 2.3.1. Animal care and experimental design

Thirty-six male SPF C57BL/6 mice (6 weeks old) were purchased from Beijing Vital River Laboratory Animal Technology Co., Ltd (Beijing China) and maintained for adapting to the new environment (24 ± 1 °C) for one week. All experiments were performed under the supervision of the Ethics Committee for Animal Experiment at Sichuan Agricultural University (Confirmation number: DYXY141642008).

As shown in Fig. 1, mice were randomly divided into 6 groups, with 6 mice in each group. The mice were pre-administrated with the commercial drug Mesalazine Enteric Coated Tablets (containing mainly anti-

inflammatory 5-aminosalicylic acid, Sunflower Pharmaceutical Industry Co. Ltd, China), as the positive control, or different dosages of AL-I for 14 days (D1 to D14, dissolved in germ-free distilled water) by gastric gavage. One week after administration, 2.5 % (w/v) of dextran sodium sulfate (DSS) (dissolved in germ-free distilled water, with *Mw* 36,000–50,000 Da, MP Biomedicals, Ontario, CA, United States) was used to induce acute ulcerative colitis [17], given through drinking water for 7 days (from D8 to D14). The mice with no treatment of DSS during the whole experimental period was set as negative control (control group), while those treated only with DSS was set as colitis control (model group). Body weight, stool characteristics and the presence of occult blood in the feces were recorded daily after DSS was given (D8 to D14), by which the disease activity index (DAI) was calculated according to an evaluation system (Table S1) [18]. 24 h after the last administration, mice were euthanized with carbon dioxide followed by cervical dislocation, and blood, cecal content and colonic tissues were collected. Colon length was measured immediately before being collected, as shown in the following sections.

#### 2.3.2. Determination of myeloperoxidase (MPO) level and secretions and gene expressions of pro-inflammatory cytokines

Colon tissues were ground under liquid nitrogen (N<sub>2</sub>). 40 mg of tissues were homogenized in 2 mL Phosphate Buffered Saline (PBS, 1 ×), centrifuged at 1500g for 15 min, and the supernatants were used for the analysis of secretions of MPO, IL-1β, IL-6, and TNF-α by ELISA kits according to manufacturer's instructions. Serum cytokine IL-1β, IL-6 and TNF-α, as well as the levels of LPS, were also quantified by ELISA kits.

Around 10 mg of colon tissues were used for the analysis of gene expressions of NOD and TLR4 receptors and tight junction proteins by qRT-PCR. Briefly, total RNA of colonic tissues was isolated using Trizol Reagent (Biomed, RA101-12, China), and reverse transcribed into cDNA using M-MLV 4 First-Strand cDNA Synthesis Kit (Biomed, RA101-12, China). All real-time PCR analysis were performed by SYBR Premix Ex Taq™ II (Tli RNaseH Plus) (Mei5Bio, China), and the gene expressions were quantified as relative regulation fold compared with *β-actin* (normalizing reference). Primers are shown in Table S2.

#### 2.3.3. Histological evaluation

After fixation with 4 % paraformaldehyde solution for more than 24 h, paraffin slices (4 μm) of colon tissues were cut and stained with hematoxylin and eosin (H&E). The colon slices were further analyzed in a blinded fashion, and the histological assessment index (HAI) was scored according to the evaluation system listed in Table S3 [18]. Brightfield images at 200 × magnification were captured on Nikon Eclipse Ti microscope (Melville, NY, USA).

#### 2.3.4. Analysis of short-chain fatty acids (SCFAs) and branched-chain fatty acids (BCFAs) in the cecal content

The content of SCFAs, including acetic, butyric, and propionic acids, and BCFAs such as isovaleric and isobutyric acids of cecum content were analyzed by GC based on methods described previously [19] with minor modifications. See details for sample preparation and GC in supplementary methods. Crotonic acid (internal standard) and standards were used as shown in Table S4.

#### 2.3.5. Serum untargeted metabolomics analysis

Fresh serum samples (100 μL) were analyzed by Novogene Co., Ltd. (Beijing, China) for a host metabolomic study. Briefly, processed samples were injected into an LC-MS/MS system with a Vanquish UHPLC system (ThermoFisher, Germany) and were processed using the Compound Discoverer 3.1 (CD3.1, ThermoFisher). All metabolites were identified with mzCloud (<https://www.mzcloud.org/>), mzVault and MassList, and annotated using the Kyoto Encyclopedia of Genes and Genomes (KEGG) (<https://www.genome.jp/kegg/pathway.html>), HMDB (<https://hmdb.ca/metabolites>) and LipidMaps (<http://www.lipidmaps.org/>) databases. Principal Components Analysis (PCA) and

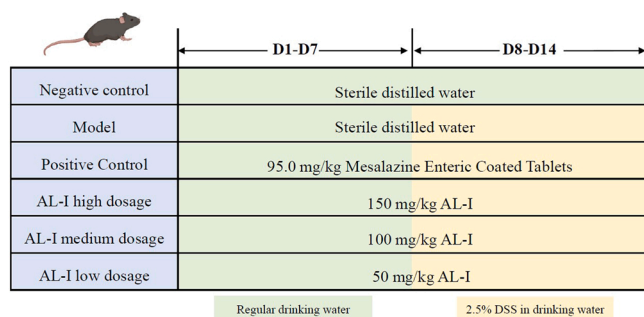


Fig. 1. Schematic overview of experimental design. Mesalazine and AL-I were given by gastric gavage.

Partial Least Squares Discriminant Analysis (PLS-DA) were performed by metaX. The functions of these metabolites and metabolic pathways were screened in the KEGG database. Details can be found in [supplementary methods](#).

2.3.6. Gut microbiota analysis

Fresh feces of mice were processed and analyzed by Beijing Novogene Science and Technology Co., Ltd, as predicted in [supplementary](#)

[material](#). Briefly, the 16 S rRNA genes of the V4 regions were amplified from feces genome, and were further sequenced and analyzed. Sequences with  $\geq 97\%$  similarity were assigned to the same operational taxonomic units (OTUs). Alpha and beta diversity analysis were used to evaluate microbiota diversity and differences. Cluster analysis was performed by PCA, principal coordinate analysis (PCoA) and non-metric multi-dimensional scaling (NMDS) by R software. Different and enriched bacterial species among groups were analyzed by MetaStat and

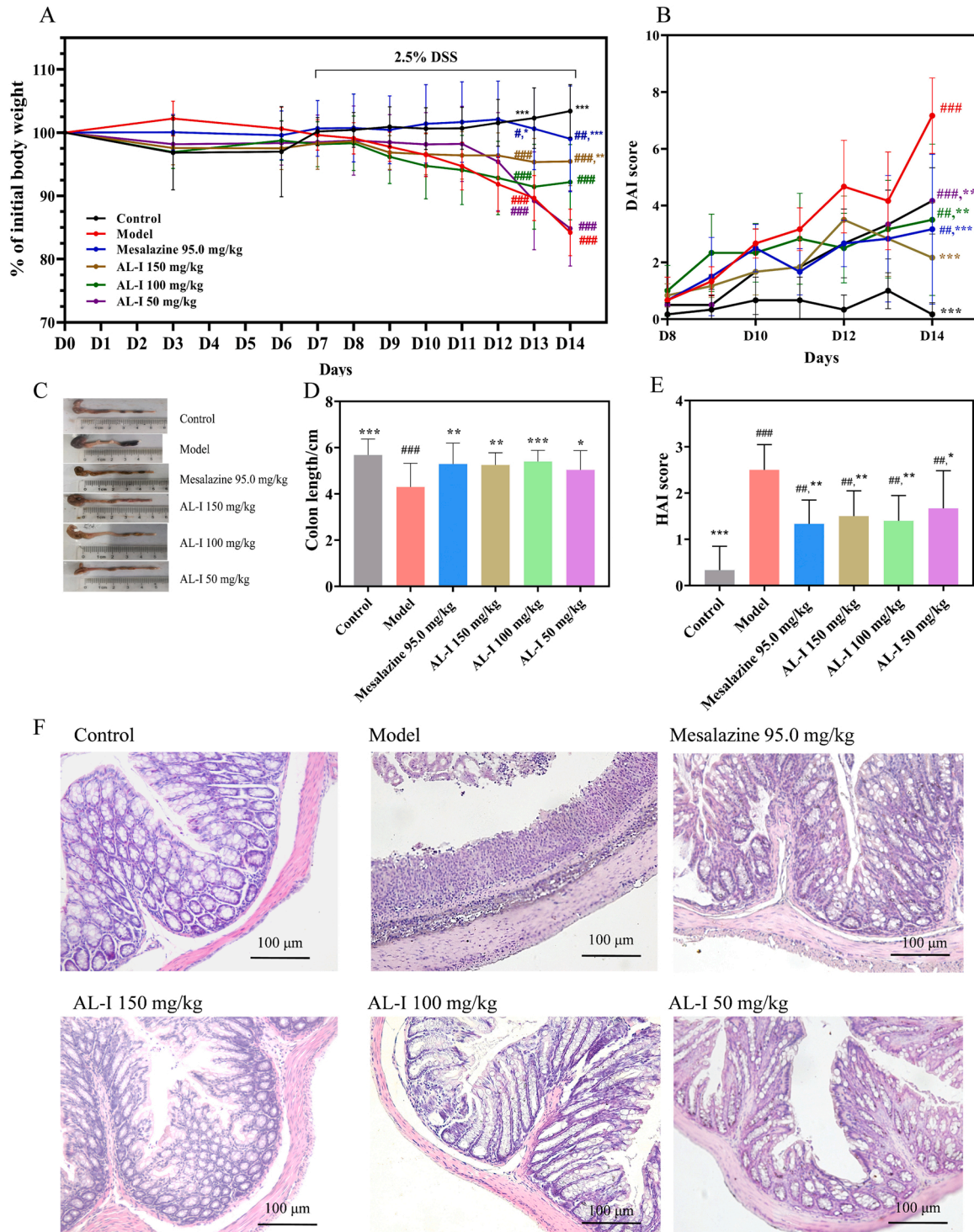


**Fig. 2.** Effects of AL-I on body weight (A, D1 to D14), DAI scores (B, D8 to D14), colon tissues (C, D14) and lengths (D, D14), HAI scores (E, D14) and histological changes (F, D14) of DSS-induced ulcerative colitis mice. #  $p < 0.05$  versus control group; ##  $p < 0.01$  versus control group; ###  $p < 0.001$  versus control group; \*  $p < 0.05$  versus model group; \*\*  $p < 0.01$  versus model group; \*\*\*  $p < 0.001$  versus model group;  $n = 6$ .

LDA effect size (LEfSe) with statistical analysis of t-test.

#### 2.4. Statistical analysis

Besides the statistical analysis used in metabolomic and microbiota experiments, the rest of data were expressed as the mean  $\pm$  S.D. and analyzed using one-way ANOVA analysis of variance and LSD test (IBM SPSS Statistics version 24, IBM Corp., Armonk, New York, USA). #,  $p < 0.05$  versus control group; ##,  $p < 0.01$  versus control group; ###,  $p < 0.001$  versus control group; \*,  $p < 0.05$  versus model group; \*\*,  $p < 0.01$  versus model group; \*\*\*,  $p < 0.001$  versus model group; ns, no significant difference was observed.

### 3. Results and discussion

#### 3.1. Isolation, chemical composition and molecular weight determination of AL-I

A crude polysaccharide from *A. Carmichaelii* leaves, ALP, was isolated after water extraction and ethanol-precipitation, and an acidic fraction AL-I was further obtained after anion exchange chromatography [5]. A

protein content of 1.0 % was determined in AL-I, while no phenolic compounds were found. It was further shown that AL-I was composed of mainly galacturonic acid (GalA, 50.3 mol%), followed by arabinose (Ara, 15.1 mol%), galactose (Gal, 14.3 mol%), xylose (Xyl, 6.9 mol%), rhamnose (Rha, 6.3 mol%), and minor amounts of glucose (Glc, 2.9 mol%), glucuronic acid (GlcA, 1.9 mol%), fucose (Fuc, 1.2 mol%) and mannose (Man, 1.0 mol%) (Fig. S1). AL-I could consist of typical pectic polysaccharide units due to the high amount of GalA and the presence of Rha which are the main monomers in type I rhamnogalacturonan (RG-I) domains [20]. This is consistent with previous results showing that AL-I was composed of pectic polysaccharides where Gal and Ara could be due to the pectic structural elements arabinogalactans, galactans and/or arabinans [5]. Additionally, AL-I was shown to be a fraction with wide range *M<sub>w</sub>*, from 26 kDa to 270 kDa, after determination on size exclusion chromatography packed with Superose 6.

#### 3.2. AL-I protected ulcerative colitis mice from severe colitis symptoms

Compared with mice in the control group, a significant reduction of bodyweight (Fig. 2A), increase in DAI index (Fig. 2B), and shortening of colonic lengths in the model group (Fig. 2C–D) indicated that the

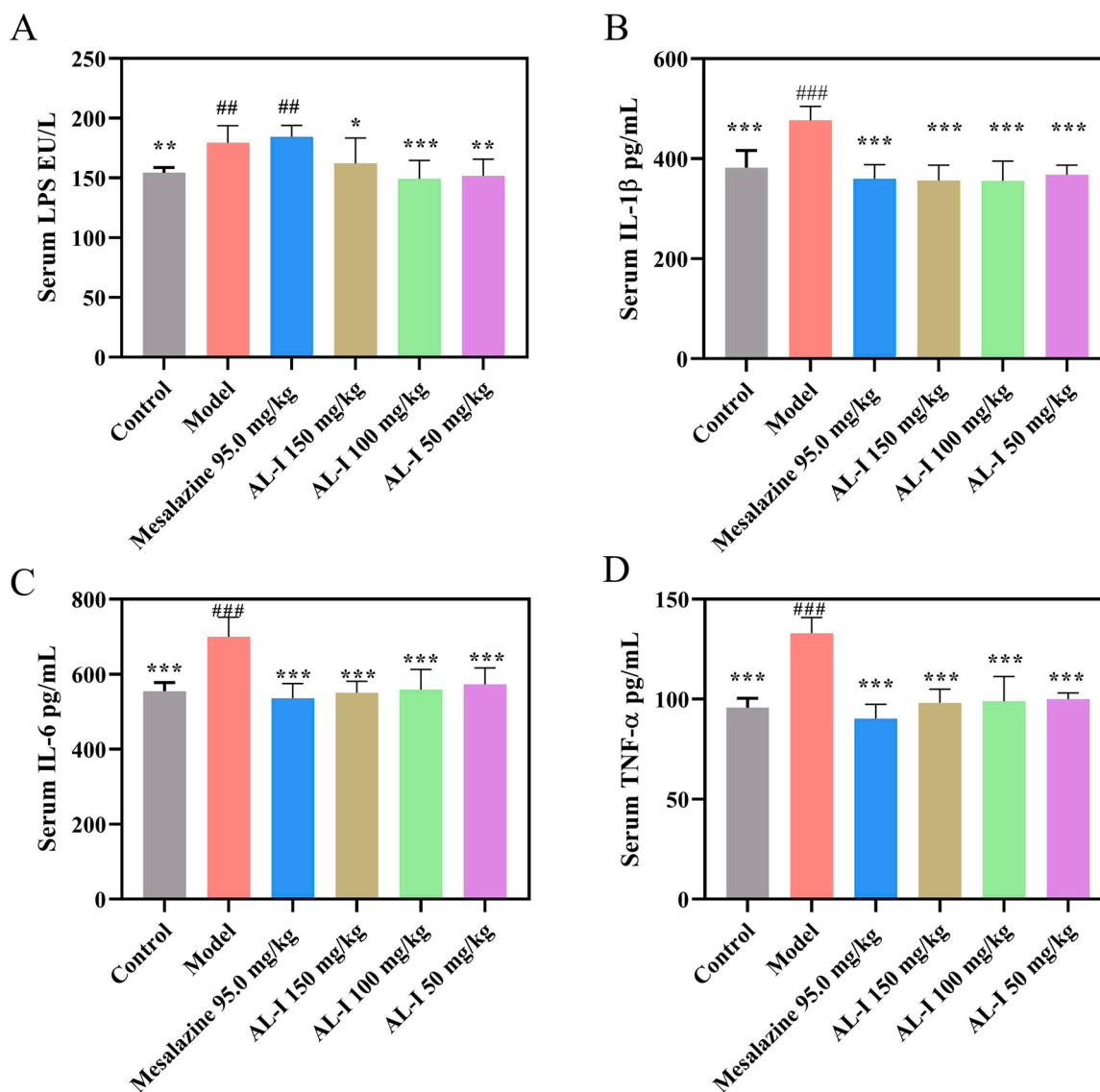


**Fig. 3.** Effects of AL-I on serum LPS (A), IL-1 $\beta$  (B), IL-6 (C) and TNF- $\alpha$  (D) of DSS-induced ulcerative colitis mice. #  $p < 0.05$  versus control group; ##  $p < 0.01$  versus control group; ###  $p < 0.001$  versus control group; \*  $p < 0.05$  versus model group; \*\*  $p < 0.01$  versus model group; \*\*\*  $p < 0.001$  versus model group; n = 6.

ulcerative colitis model in mice was successfully established, as described in a previous study [17,21]. The obvious damage on colonic surface epithelium, crypt and mucosal structure, and increased infiltration of inflammatory cells also proved colitis severity caused by DSS (Fig. 2F). After oral administration of 50, 100 or 150 mg/kg AL-I, these symptoms of colitis mice were ameliorated. This was especially observed on D14 when both the body weight and DAI index were statistical significantly reversed by AL-I treatment ( $p < 0.01$ ) compared to the model mice, as presented in Figs. 2A and 2B. Similar restorative effects also occurred in mice treated with the positive control Mesalazine (Fig. 2C–F). The HAI scores according to colonic histological observations also gave a clear indication for these restorations by AL-I and Mesalazine (Fig. 2E). No change was observed in body weight (Fig. 2A) of mice before DSS intervention.

The levels of serum pro-inflammatory cytokines IL-1 $\beta$ , IL-6, and TNF- $\alpha$  were notably elevated in colitis mice, but the levels in mice supplemented with all doses of AL-I were considerably lower ( $p < 0.001$ ), being close to normal levels (no significant difference with the control group) (Fig. 3B–D). A rising secretion of serum LPS is one of the indicators of systematic inflammation of colitis mice ( $p < 0.001$ ), but this was relieved in all AL-I groups ( $p < 0.001$ ) (Fig. 3A). Therefore, it was demonstrated that AL-I intervention at different dosages were able to protect against colitis-associated symptoms and attenuate inflammation in DSS-induced ulcerative colitis mice.

### 3.3. AL-I ameliorated colonic inflammation and repaired gut barrier function in DSS-induced ulcerative colitis mice

As a local mediator of tissue damage and the resulting inflammation in various inflammatory diseases and ulcerative colitis [21,22], the amount of MPO in colon tissues was significantly enhanced in the model group, which revealed a severe inflammatory reaction in the colon of ulcerative colitis mice [22]. It was however dramatically reversed by all doses of AL-I ( $p < 0.001$ ) (Fig. 4A). Similar inhibition on the secretions of IL-1 $\beta$ , IL-6 and TNF- $\alpha$  (Fig. 4A) were also observed in all AL-I-treated mice. The down-regulations of these inflammatory mediators could be due to the inhibition of AL-I on activation of pattern-recognition receptors (PRRs), such as nucleotide-binding oligomerization domain 1 (NOD1) and Toll-like receptor 4 (TLR4) on the surface of intestinal epithelial cells, evidenced by the reduced colonic mRNA expressions of these receptors compared to model group (Fig. 4B). These receptors could be the possible active sites of AL-I for its anti-inflammatory effects, as shown by other pectic polysaccharides [11,12,20].

Upon epithelial injury, a damaged intestinal mucosal integrity by DSS is one of the causes of intestinal inflammation [17]. An observed

increase of serum LPS suggested a possible invasion of endotoxin after intestinal mucosa injury (Fig. 3A), as well as down-regulation of colonic tight junction (TJ) proteins such as ZO-1 and occludin (Fig. 4B) that are crucial to protect the intestinal epithelial barrier. However, gene expressions of both ZO-1 and occludin were improved after 14-day treatment of AL-I (Fig. 4B), being equivalent to those reported for other natural polysaccharides [10,23–25]. These results suggest that AL-I administration could protect mice from reduced intestinal barrier functions by promoting the expressions of TJ proteins.

### 3.4. AL-I promoted production of SCFAs and BCFAs in DSS-induced ulcerative colitis mice

Total SCFAs, acetic acid, and isovaleric acid have been reported as the main fermentation products of water-soluble polysaccharides, and exhibit immunomodulatory effects and are involved in intestinal protection [20,26,27]. The BCFAs isovaleric acid and isobutyric acid are metabolic end products of undigested protein when fermentable fiber supply decrease, but are generally omitted as they are present in lower quantities than SCFAs [28]. After DSS induction, the contents of total SCFAs, acetic acid, and isovaleric acid visibly decreased ( $p < 0.05$ ) compared to the control group (Fig. 5), whereas in mice administered with AL-I the contents were significantly restored in a dosage-dependent manner, with acetic acid being the predominant one promoted by AL-I. These changes could be another explanation for the protective activities of AL-I on colitis mice, as SCFAs can play a key role in the protective activities of colitis mice through anti-inflammatory effects, regulation of the differentiation of intestinal epithelial cells and maintenance of intestinal barrier [20,27]. Additionally, BCFAs may serve as alternative fuels in colonocytes [29], which could potentially be an indirect way for the activity of AL-I. Comparatively, the contents of these SCFAs were not affected by the chemical therapeutic medication Mesalazine. The production of SCFAs has been reported to be dramatically reduced in colitis mice, probably due to less bacterial diversity and reduction of abundance of SCFAs-producing bacteria [20,27]. Thus, an underlying balance of AL-I on DSS-induced dysbiosis might also contribute to its modulatory effects on SCFAs, as well as other positive reactions on colitis.

### 3.5. AL-I modulated host metabolomics in DSS-induced ulcerative colitis mice

For a better understanding of the active mechanism of AL-I, an untargeted metabolomics analysis was performed to discover the potential metabolites and pathways that are affected by AL-I (150 mg/kg)

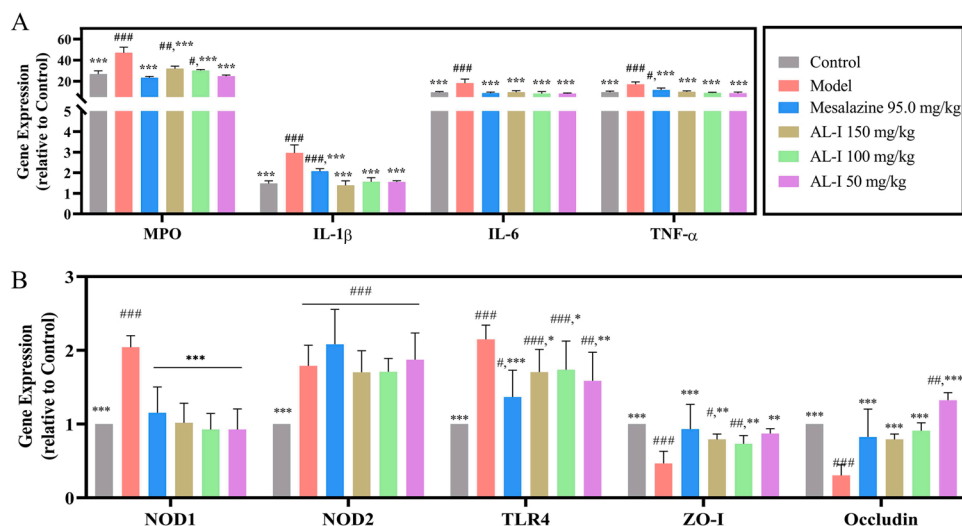


**Fig. 4.** Effects of AL-I on colonic inflammation and barrier functions of DSS-induced ulcerative colitis mice. Colonic MPO levels and secretions of the pro-inflammatory cytokines IL-1 $\beta$ , IL-6 and TNF- $\alpha$  were determined using ELISA kits (A); Gene expressions of inflammatory signal receptors and tight junction proteins were quantified using qRT-PCR (B). #  $p < 0.05$  versus control group; ##  $p < 0.01$  versus control group; ###  $p < 0.001$  versus control group; \*  $p < 0.05$  versus model group; \*\*  $p < 0.01$  versus model group; \*\*\*  $p < 0.001$  versus model group; ns, no significant difference; n = 6.

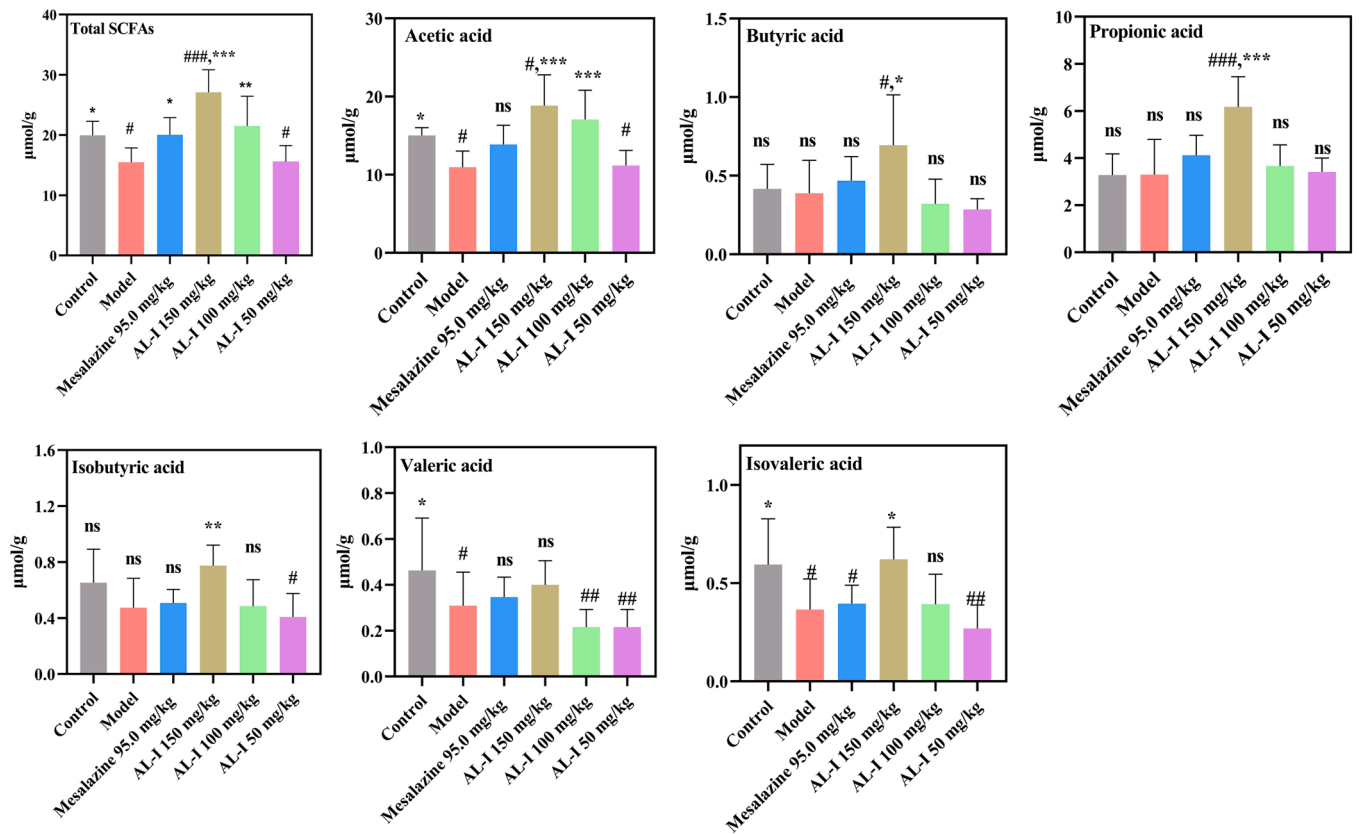


Fig. 5. Effects of AL-I on concentrations of SCFAs and BCFAs in cecum content. #  $p < 0.05$  versus control group; ##  $p < 0.01$  versus control group; ###  $p < 0.001$  versus control group; \*  $p < 0.05$  versus model group; \*\*  $p < 0.01$  versus model group; \*\*\*  $p < 0.001$  versus model group; ns, no significant difference; n = 6.

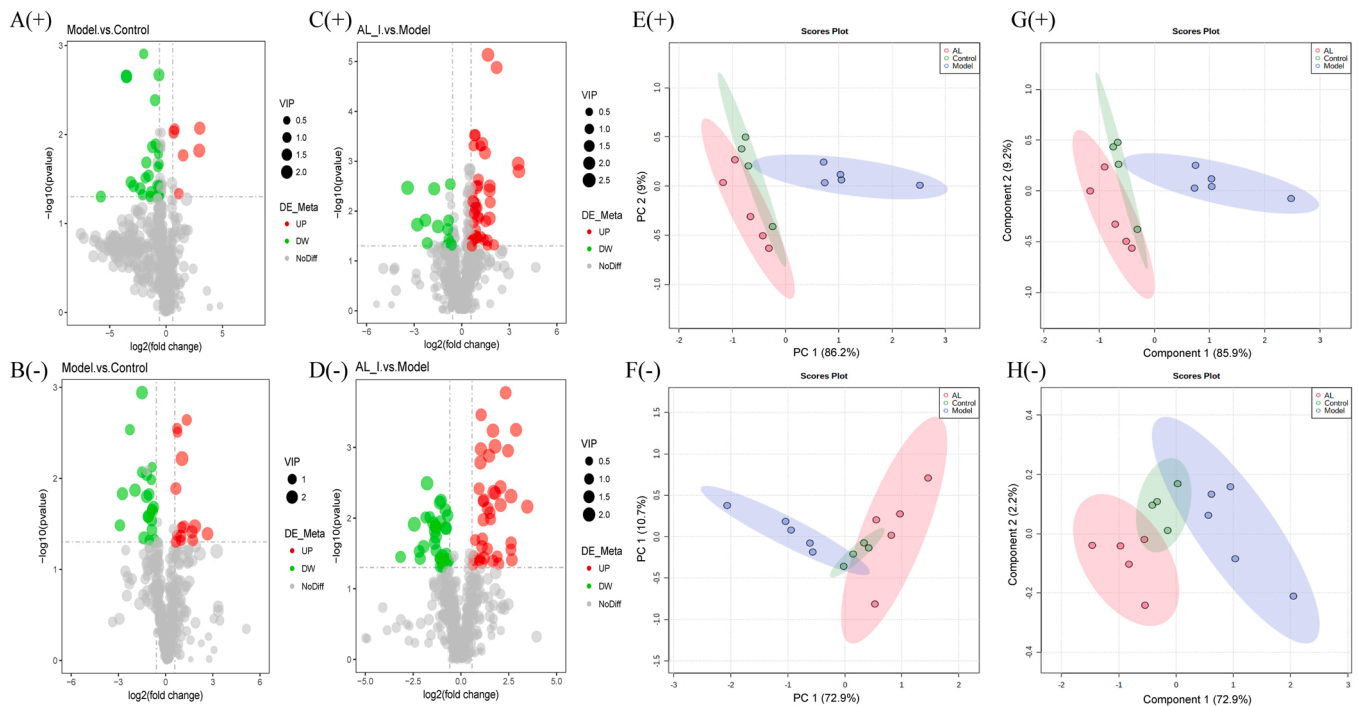


Fig. 6. Effects of AL-I on serum metabolomic profile of DSS-induced ulcerative colitis mice. Volcano plots in positive mode (+, A, C) and negative mode (-, B, D) altered within groups. PCA and PLS-DA analysis of modulated differential metabolites in positive (+, E, G) and negative mode (-, F, H), respectively. AL/AL\_I represents the AL-I 150 mg/kg group, Model represents model mice treated with DSS only, and Control represents control mice without treatment.

on colitis mice. Generally, 656 metabolites in positive ionization mode (+) and 469 in negative mode (-) were identified and quantified based on mzCloud, mzVault, and MassList database (Table S5). Considerable differences in total (Fig. S2) and differential metabolites among groups (Fig. S3) were observed after PCA and PLS-DA analysis. Metabolites with significant up- or down-regulation within groups were further chosen (Table S5, Fig. 6A–D) after PCA (Fig. 6E, F) and PLS-DA (Fig. 6G, H) analysis. Herein, 8 (+) and 19 (-) metabolites were altered by AL-I compared to the model and control groups (Fig. 7). Every differential metabolite was verified for accuracy by receiver operating characteristic (ROC, not shown).

Relevant metabolites and the included metabolic pathways are listed in Table S6 after screening in KEGG database. In positive mode, the nicotinate and nicotinamide metabolism ( $p = 0.001$ ) and porphyrin and chlorophyll metabolism ( $p = 0.005$ ) pathways were suppressed by DSS (Table S6, Fig. 8A), represented by the alterations of nicotinamide and biliverdin (Fig. 8G) respectively. However, AL-I failed to restore the levels of these metabolites and their included pathways, except modulation on the glycerophospholipid metabolism compared to both model and control groups (Fig. 8C, E). In negative mode, 5 pathways were tentatively found to be affected by DSS compared to normal mice (Fig. 8B) and were further significantly restored by AL-I compared with the model group, including the pentose phosphate pathway ( $p = 0.036$ , enriched with D-erythrose 4-phosphate and D-sedoheptulose 7-phosphate), fructose and mannose metabolism ( $p = 0.019$ , enriched with D-mannose 6-phosphate and dihydroxyacetone phosphate), amino sugar and nucleotide sugar metabolism ( $p = 0.018$ , enriched with D-mannose 6-phosphate), purine metabolism ( $p = 0.001$ , enriched with uric acid, xanthosine, and 2,6-dihydroxypurine) and the biosynthesis of unsaturated fatty acids pathway ( $p = 0.011$ , enriched with linoleic acid, arachidonic acid, 8Z,11Z,14Z-eicosatrienoic acid, docosahexaenoic acid

and eicosapentaenoic acid), as shown in Fig. 8D, H and Table S6. In addition, the linoleic acid metabolism and arachidonic acid metabolism (Fig. 8D–F) pathways were inhibited by AL-I represented mainly by linoleic acid (Table S6 and Fig. 8H).

The pentose phosphate pathway is a fundamental component in cellular metabolism, which is crucial for maintaining carbon homeostasis, nucleotide, and amino acid biosynthesis, as well as defeating oxidative stress [30]. The levels of two constituents in the non-oxidative branch of this pathway, D-erythrose 4-phosphate, and D-sedoheptulose 7-phosphate were promoted after AL-I treatment (Fig. 8H), which suggested a possible modulatory effect of AL-I on the transaldolase-catalysed reaction. The process of mannose 6-phosphate generation, a metabolite included in the fructose and mannose metabolism and amino sugar and nucleotide sugar metabolism, has been proposed to inhibit IL-1 $\beta$  production in macrophages via suppressing glycolysis by reducing glucose 6-phosphate [31]. It is also responsible for the inhibition of TLR4 expression and suppression of the inducible nitric oxide synthase (iNOS) expression and NO and cytokine production, by competitively binding with insulin-like growth factor II/mannose-6-phosphate (IGF-II/M6P) receptor [32]. Therefore, the significantly increased mannose-6-phosphate might be one of the contributors to the anti-inflammatory effect of AL-I. Lipids derived from polyunsaturated fatty acids, such as arachidonic acid, eicosapentaenoic acid, and docosahexaenoic acid, are not only functioning as anti-inflammatory activators but also act as immunomodulators and signaling molecules (in the family of prostanoids) to drive some of the signs of inflammation. They can be activated and released from cell membrane phospholipid stores when stimuli such as a microorganism or damage appear [33]. The levels of these metabolites increased in colitis mice both in current and previous studies [34,35], and AL-I suppressed their levels (Fig. 8H), as well as their associated metabolic pathways

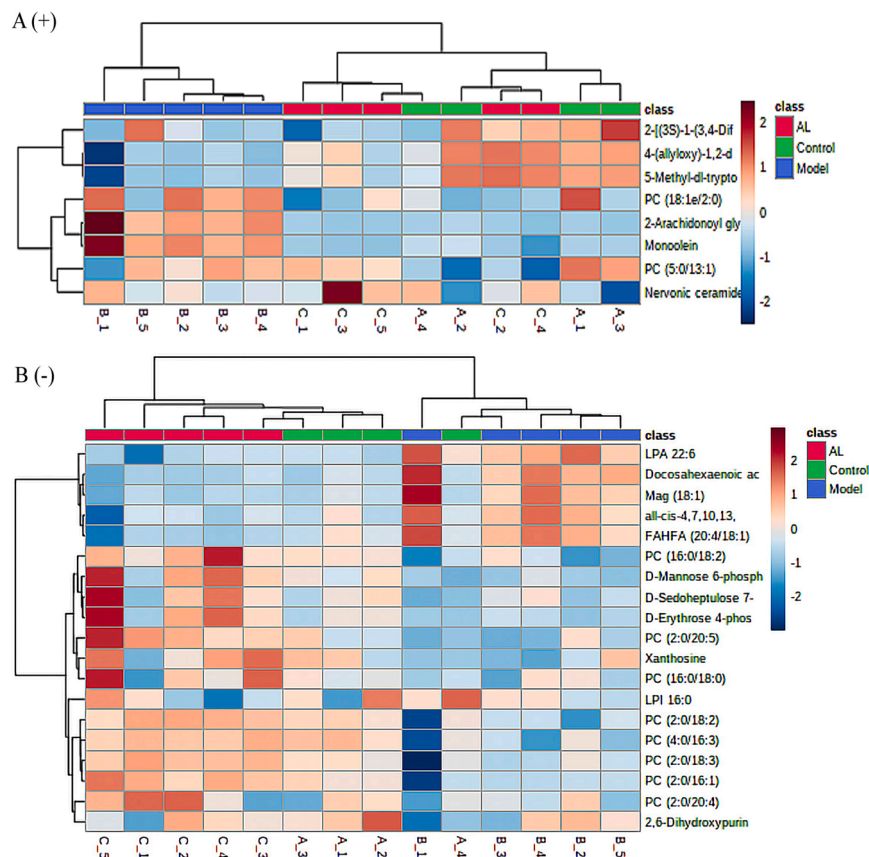


**Fig. 7.** Clustered heatmaps of modulated differential metabolites within three groups in positive mode (+, A) and negative mode (-, B). AL represents the AL-I 150 mg/kg group, Model represents model mice treated with DSS only, and Control represents control mice without treatment.

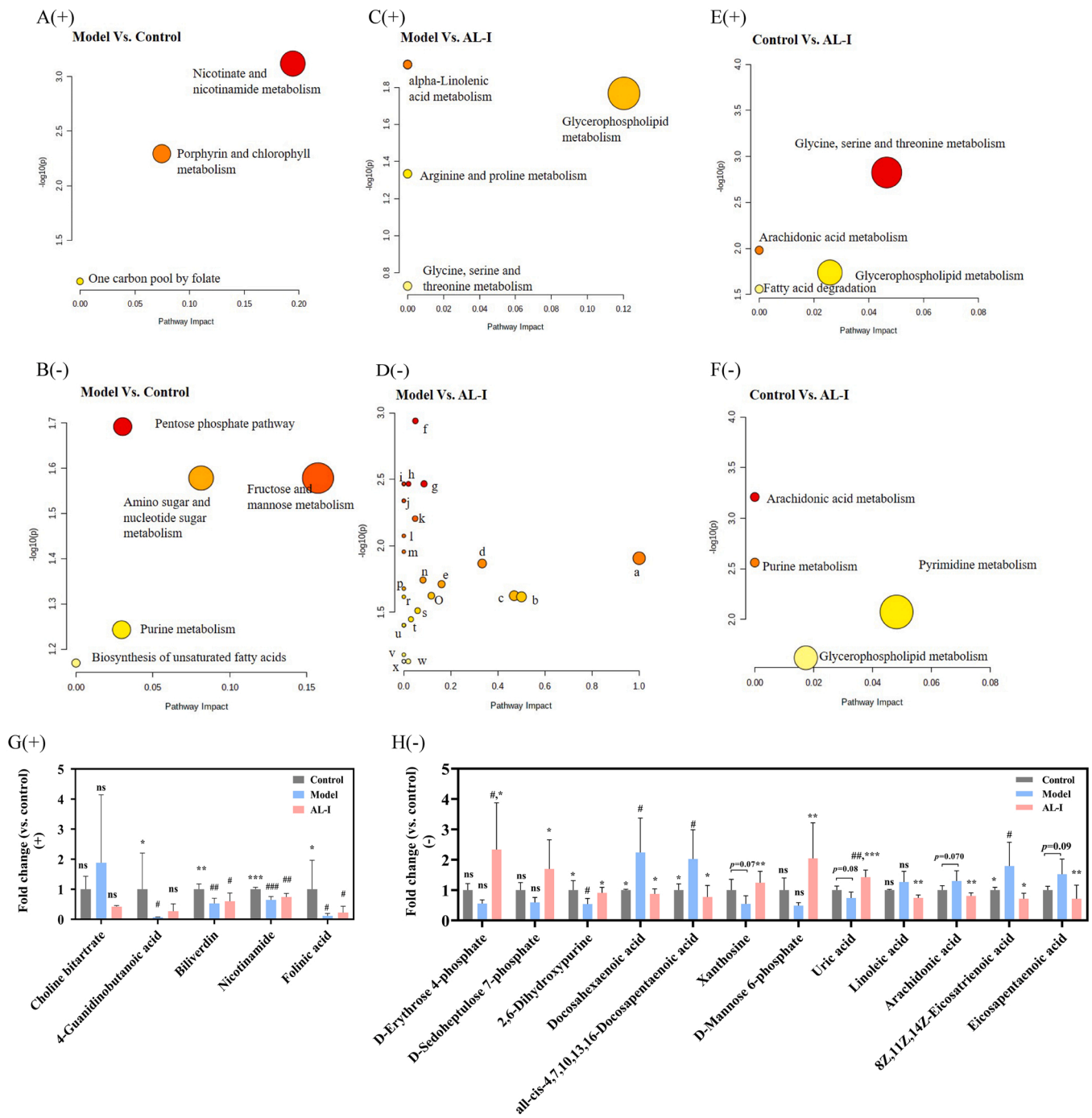


**Fig. 8.** Effects of AL-I on metabolic pathways and metabolites of DSS-induced colitis mice. Pathways were concluded based on metabolites in both positive (+) and negative (-) modes, and analyzed between model vs control (A, B), model vs AL-I (C, D) and control vs AL-I (E, F). Detailed metabolic pathways of (D) are: a, Linoleic acid metabolism; b, D-glutamine and D-glutamate metabolism; c, Alanine, aspartate and glutamate metabolism; d, Arachidonic acid metabolism; e, Fructose and mannose metabolism; f, Purine metabolism; g, Arginine and proline metabolism; h, Glutathione metabolism; i, Nitrogen metabolism; j, Aminoacyl-tRNA biosynthesis; k, Pyrimidine metabolism; l, Pentose and glucuronate interconversions; m, Biosynthesis of unsaturated fatty acids; n, Amino sugar and nucleotide sugar metabolism; o, Arginine biosynthesis; p, Steroid hormone biosynthesis; q, Butanoate metabolism; r, Citrate cycle (TCA cycle); s, Pentose phosphate pathway; t, Pantothenate and CoA biosynthesis. Specific metabolites in positive (G) and negative mode (H) are included in the metabolic pathways above. AL-I represents the AL-I 150 mg/kg group, Model represents model mice treated with DSS only, and Control represents control mice without treatment.

(Fig. 8D, Table S6). Linoleic acid is also a biomarker for the development of colitis into colorectal cancer [35], which was successfully reduced by AL-I in the current study. Collectively, these results suggested that the protection of AL-I from a disordered broad-scale metabolism process is a potential mechanism of its protective role in colitis.

Decreased levels of uric acid, 2,6-dihydroxypurine, and xanthosine were observed in the colitis mice (Fig. 8H). However, it is still

controversial whether they are related to colitis development. Serum uric acid, for instance, was previously indicated to be associated with ulcerative colitis patients having higher levels compared to healthy people [36]. However, the disease activity index of ulcerative colitis was not related with the uric acid level [37]. Moreover, 2,6-dihydroxypurine and xanthosine have also been previously reported to decrease in DSS-induced colitis mice [38]. It is consequently still a challenge to



distinguish whether these metabolites would induce or alleviate inflammatory processes in the current study, as the inflammatory threshold levels in ulcerative colitis mice remain unclear. Meanwhile, since gut dysbacteriosis was noticed not only participating in the pathogenesis of intestinal bowel diseases, but also affecting the metabolic pathways of urate [36], the change in microbiota composition might be a possible reason for the uric acid increase. A statistical modulation of serum uric acid compared to normal mice was only observed in AL-I-treated mice rather than in colitis model mice without any treatment (Fig. 8H), which also indicates that uric acid may have a greater relationship with microbiota modulation, rather than the metabolic pathways or inflammatory status, which will be discussed after the analysis of bacterial composition.

### 3.6. AL-I modulated the gut dysbiosis on DSS-induced ulcerative colitis mice

#### 3.6.1. Alpha and beta diversity analysis

Gut microbiota dysbiosis has been considered as one of the factors in ulcerative colitis development [7]. After DSS induction for 7 days, the indices of the alpha diversity of ulcerative colitis mice (model group) were significantly reduced compared to normal mice (control group) (Table S7), which indicated a decrease of microbiota diversity caused by DSS. However, alpha diversity indices of the mice treated with AL-I were significantly lower than the control group ( $p < 0.05$ ) and no difference with colitis mice was observed. It was consequently shown that 14 days of AL-I treatment had not reversed the reduced richness and diversity of microbial communities caused by DSS. The rarefaction curve (Fig. S4A) and rank abundance curve (Fig. S4B) also suggested a lower abundance of microbiota diversity in model and AL-I groups compared to the

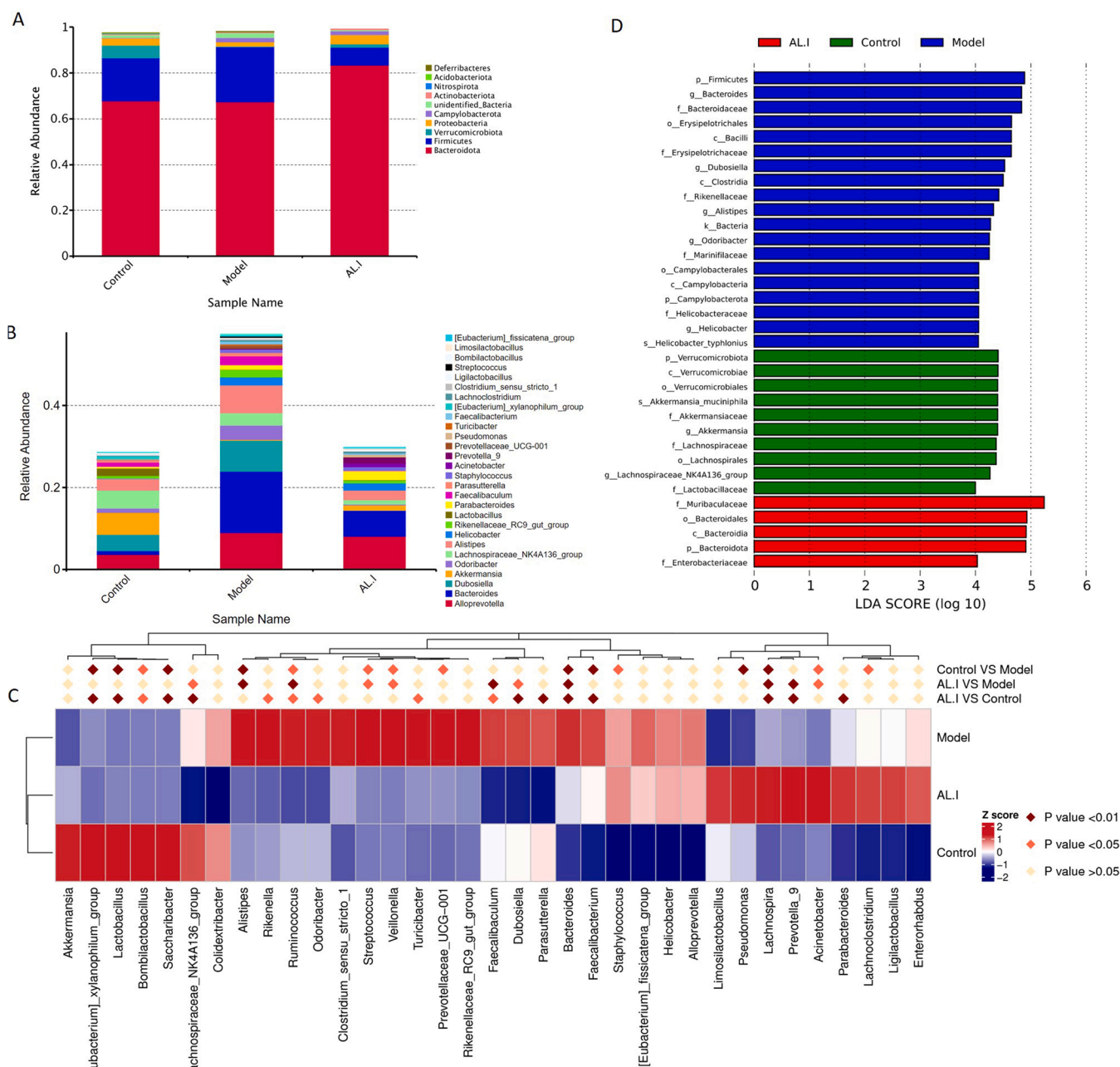


**Fig. 9.** Microbiota compositions at phylum (A) and genus levels (B) and MetaStat (C, genus) and LEfSe (D) analysis of bacterial changes of DSS-induced ulcerative colitis. AL-I represents the AL-I 150 mg/kg group, Model represents model mice treated with DSS only, and Control represents control mice without treatment.

control group. In addition, beta diversity is utilized to compare the microbiota composition among groups based on the OTUs abundance and annotation. Clear separations were observed between the control and model groups in PCoA (Fig. S4C) and PCA analysis (Fig. S4D), and NMDS analysis (Fig. S4E), which also demonstrated a huge modulation in species composition after DSS induction. Clear shifts between the model group and AL-I treated group was also observed in PCoA and NMDS analysis (Fig. S4D,E), indicating that a significant change in gut microbiota composition occurred after administration of AL-I.

### 3.6.2. Modulation of microbiota composition

The statistical difference in microbiota composition between groups was determined by Anosim and MRPP analysis (Table S7). The relative abundance of phylum, class, order, family, genus and species levels are shown in Fig. 9A, Fig. S5A–C Fig. 9B and Fig. S5D, respectively. The significantly different bacteria among groups on phylum and genus levels were further investigated by MetaStat (Fig. 9C, Fig. S6A) and LEfSe (Fig. 9D) analysis in order to determine the different bacterial species present among three groups.

*Bacteroidota*, *Firmicutes*, *Verrucomicrobiota*, *Proteobacteria* and *Camphylobacterota* are the dominant phyla in the samples (Fig. 9A), and modulation of the microbiota composition was observed both in the model group and AL-I treated group. The relative abundance of *Bacteroidota* and *Firmicutes* in the model group was not affected by DSS treatment (Fig. 9C,  $p > 0.05$ ). However, as shown in Fig. S6A and Fig. 9A, the abundance of *Acidobacteriota* and *Nitrospirota* were significantly decreased in the model group ( $p < 0.05$ ). A different pattern of microbiota composition was found in AL-I-treated colitis mice, with a more relative abundance of *Bacteroidota* ( $p < 0.05$ ), and less *Firmicutes*, *Verrucomicrobiota*, *Acidobacteriota* and *Deferribacteres* ( $p > 0.05$ ) (Fig. 9A and Fig. S6A). The imbalance of different phyla in ulcerative colitis is variable across studies, however, a decrease in the abundance of *Bacteroides* spp has also been observed in ulcerative patients [7,39] and in experimental mice [40,41]. From the aspect of pectin degradation, the *Bacteroidetes* are generally regarded as the more dominant plant polysaccharide degraders in the human gut, and the relative contribution of *Bacteroidetes* versus *Firmicutes* for the in-situ pectin degradation is yet unclear [26].

For a better understanding of the modulatory effect of AL-I on colitis microbiota, changes at the dominant genus level were further analyzed. As shown in Fig. 9B and C, 16 bacterial genera were significantly regulated in the model group compared to the control group. Some of them that had been promoted by DSS were reduced significantly by AL-I administration, including the *Bacteroides*, *Alistipes*, *Streptococcus* and *Ruminococcus* genera, and some that were inhibited by DSS were promoted by AL-I such as *Acinetobacter*, *Prevotella* 9 and *Lachnospira* (Fig. 9C). *Bacteroides*, *Dubosiella* and *Alistipes* were enriched in the model group, as shown in the LEfSe analysis (Fig. 9D). *Muribaculaceae*, belonging to the *Bacteroidetes* phylum, was mostly enriched in AL-I treated group (Fig. 9D, Fig. S5C), which might explain the higher relative abundance of *Bacteroidetes* phylum than those of the model group. Noticeably, *Bacteroides* and *Alistipes* genera were dramatically reduced by AL-I compared to the model group (Fig. 9C), and all of them belong to the *Bacteroidetes* phylum.

The above-mentioned bacterial species altered by AL-I might contribute to the protective effects on colitis. One of the top 10 bacterial genus *Bacteroides* is known to play a central role in the degradation of a wide range of plant polymers in the gut intestine and to possess a wide range of carbohydrate active enzymes in their genomes. However, they can also break down the host-derived mucin glycans, the major constituent in the intestinal mucosal layer [42], and have been suggested to be correlated with colitis [7,39,43]. *Dubosiella* has seldom been studied and its biological properties is still unclear. It has been reported with a positively correlation with butyric acid production and might be a potentially beneficial bacterial agent against colitis because of its lower richness in colitis mice than in normal ones [44]. However, a contrary

result was recently observed with higher relative abundance in DSS-induced colitis than the normal ones [45]. Therefore, the function of *Dubosiella* on colitis and other intestinal inflammation should be further investigated by more in vivo studies. Similarly, the commonly considered beneficial bacteria *Ruminococcus* has also been observed to be increased in some colitis patients [7,39]. *Alistipes* is recently discovered as a new genus of bacteria in the *Bacteroidetes* phylum, and it is still controversy around its protective and pathogenic effects [46]. For example, *A. finegoldii* was reported showing a protective effect against colitis as it was decreased in colitis mice [43], but correlations between *Alistipes* genera and colitis and colorectal cancer were also noticed [47]. In the current study, the relative abundance of *Alistipes* genera was strikingly enhanced in the model group, but was further reduced by AL-I, which is in line with a previously published study on a mannoglucan isolated from Chinese yam [48]. The abundance of *A. finegoldii* was also found to be increased after treatment with AL-I (Fig. S6B), which, to some extent, also indicated an underlying restoration of AL-I on gut microbiota to protect against colitis. These enriched bacterial genera (*Bacteroides*, *Dubosiella*, and *Alistipes*) were significantly reduced by AL-I, which could be a potential way for pectin to protect against colitis. As for the genus of *Lachnospira*, *Prevotella*, *Parabacteroides* and *Faecalibacterium* that increased by AL-I relative to either model or control group, they have been reported with fermentative ability on pectins and their relative abundance would be increased during the fermentation [49–51]. However, the relative abundance of beneficial bacteria, such as *Akkermansia* and *Lactobacillus*, in the AL-I treated group was still statistically lower than the control group (Fig. 9C), but a mild improvement in *Akkermansia* genera was observed in Fig. 9B, C. All results demonstrated that the pectic polysaccharide AL-I could significantly reverse the microbiota changes induced by DSS treatment, and suggested that these variations on the abundance of bacteria could be involved in its protective effects against ulcerative colitis.

### 3.7. Correlation between metabolomic and microbiota composition

The correlation between the different metabolites in serum and different microbiota genera was determined using correlation heatmap analysis (Fig. 10). Six metabolites that increased after AL-I treatment compared to the model mice, including L-glutamic acid, D-mannose 6-phosphate, uric acid, xanthosine, orotic acid, and D-erythrose 4-phosphate (negative mode, Table S6), were classified with certain correlations with bacterial genera. Four of them were significantly negatively correlated with *Alistipes* genera. However, the *Prevotella* and *Bacteroides*

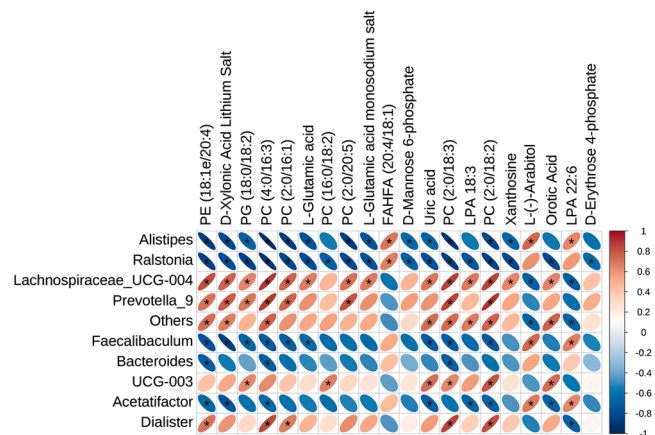


**Fig. 10.** Heatmap showing the correlation between the differentiated microbiota genera and identified metabolites. Metabolites included were the ones with significant differences between AL-I and the model group in negative ionization mode. \*, represents that the correlation within specific metabolite and bacterial species was statistically significant ( $p < 0.05$ ).

were correlated with other metabolites, such as PE (18:1e/20:4), PC (4:0/16:3) and PC (2:0/18:3). At the same time, it was noticed that the level of uric acid presented significant correlations with six bacterial genera, which further verified the forementioned speculation that the potent alteration of uric acid was related more to the microbiota composition modulated by AL-I. However, other bacteria that was promoted by AL-I had no significant correlation observed with these metabolites, which could be due to the relatively short intervention time in the current study. Long-term oral administration, as well as microbiota transplantation is needed in further research in order to investigate a clearer relation between gut microbiota and host metabolism. Moreover, the imbalance of intestinal inflammatory effector cells and regulatory cells contributes to strong activation of the immune system with increased inflammatory effector cells. This may also lead to prolonged or chronic inflammation, which is detrimental and closely associated with the development of ulcerative colitis [52,53]. For instance, the change in bacterial composition, as well as the resulting modulation on SCFAs, might be involved in the differentiation and expansion of T regulatory or Th17 cells and thereby introducing inflammatory and bacterial infection to the intestinal mucosa [52]. This would be of interest to further investigate on colitis mice, normal or germ-free mice, in order to identify the exact modulatory effects of AL-I on intestinal immune homeostasis.

#### 4. Conclusions

In this study, different dosages of a pectic type polysaccharide fraction (AL-I) isolated from *A. carmichaelii* leaves were orally administrated in DSS-induced ulcerative colitis mice and significantly ameliorated colitis symptoms, attenuated serum and colonic inflammatory indices and injury on colonic histological structure. AL-I showed a potent protective effect through inhibiting the activation of NOD1 and TLR4 receptors, promoting expressions of TJ proteins and restoring the production of SCFAs and BCFAs. In addition, metabolomic biomarkers such as  $\gamma$ -glutamic acid,  $D$ -mannose 6-phosphate, uric acid, xanthosine, orotic acid, and  $D$ -erythrose 4-phosphate were modulated by high dosage of AL-I, and the dysbiosis of gut microbiota represented by *Bacteroides*, *Alistipes*, *Streptococcus* and *Ruminococcus*, *Acinetobacter*, *Prevotella* 9 and *Lachnospira* genera were restored. These findings suggested that AL-I exert promising protection on DSS-induced ulcerative colitis mice, and that the leaves of *A. carmichaelii* have a potential to be utilized as a medicinal plant resource for the treatment of inflammatory intestinal diseases.

#### CRedit authorship contribution statement

**Yu-Ping Fu:** Data curation, Investigation, Methodology, Visualization, Writing – original draft. **Cen-Yu Li:** Data curation, Investigation, Methodology, Visualization. **Xi Peng:** Data curation, Software. **Helle Wangenstein:** Project administration, Supervision, Writing – review & editing. **Kari Tvete Inngjerdingen:** Methodology, Project administration, Supervision, Writing – review & editing. **Yuan-Feng Zou:** Funding acquisition, Methodology, Project administration, Resources, Supervision, Writing – review & editing.

#### Conflict of interest statement

The authors declare that they have no known competing financial interests or personal relationships that could have appeared to influence the work reported in this paper.

#### Acknowledgement

The first author acknowledges the funding from the China Scholarship Council (201906910066) and Sichuan Veterinary Medicine and Drug Innovation Group of China Agricultural Research System (SCCXTD-2020-18). We acknowledge the support by the Key Laboratory

of Animal Disease and Human Health of Sichuan Province, and help from Dr. Anne Grethe Hamre for the determination of monosaccharide composition. We also appreciate the helpful comments on this manuscript from Professor Emerita Berit Smestad Paulsen, Section for Pharmaceutical Chemistry, Department of Pharmacy, University of Oslo.

#### Appendix A. Supporting information

Supplementary data associated with this article can be found in the online version at doi:10.1016/j.biopha.2022.113767.

#### References

- [1] C. Huang, Z.X. Li, Y. Wu, Z.Y. Huang, Y. Hu, J. Gao, Treatment and bioresources utilization of traditional Chinese medicinal herb residues: recent technological advances and industrial prospect, *J. Environ. Manag.* 299 (2021), 113607, <https://doi.org/10.1016/j.jenvman.2021.113607>.
- [2] Chinese Pharmacopoeia Committee. *Chinese Pharmacopoeia, 2020 ed.*, Chemical Industry Press, Beijing, 2020.
- [3] Y.-P. Fu, Y.-F. Zou, F.-Y. Lei, H. Wangenstein, K.T. Inngjerdingen, *Aconitum carmichaelii* Debeaux: a systematic review on traditional use, and the chemical structures and pharmacological properties of polysaccharides and phenolic compounds in the roots, *J. Ethnopharmacol.* 291 (2022), 115148, <https://doi.org/10.1016/j.jep.2022.115148>.
- [4] Y.-N. He, S.-P. Ou, X. Xiong, Y. Pan, J. Pei, R.-C. Xu, F.-N. Geng, L. Han, D.-K. Zhang, M. Yang, Stems and leaves of *Aconitum carmichaelii* Debx. as potential herbal resources for treating rheumatoid arthritis: chemical analysis, toxicity and activity evaluation, *Chin. J. Nat. Med.* 16 (9) (2018) 644–652, [https://doi.org/10.1016/s1875-5364\(18\)30104-3](https://doi.org/10.1016/s1875-5364(18)30104-3).
- [5] Y.-P. Fu, C.-Y. Li, X. Peng, Y.-F. Zou, F. Rise, B.S. Paulsen, H. Wangenstein, K. T. Inngjerdingen, Polysaccharides from *Aconitum carmichaelii* leaves: structure, immunomodulatory and anti-inflammatory activities, *Carbohydr. Polym.* 291 (2022), 119655, <https://doi.org/10.1016/j.carbpol.2022.119655>.
- [6] R. Ungaro, S. Mehandru, P.B. Allen, L. Peyrin-Biroulet, J.-F. Colombel, Ulcerative colitis, *Lancet* 389 (2017) 1756–1770, [https://doi.org/10.1016/S0140-6736\(16\)32126-2](https://doi.org/10.1016/S0140-6736(16)32126-2).
- [7] X.Y. Guo, X.J. Liu, J.Y. Hao, Gut microbiota in ulcerative colitis: insights on pathogenesis and treatment, *J. Dig. Dis.* 21 (2020) 147–159, <https://doi.org/10.1111/1751-2980.12849>.
- [8] A. Lavelle, H. Sokol, Gut microbiota-derived metabolites as key actors in inflammatory bowel disease, *Nat. Rev. Gastroenterol. Hepatol.* 17 (2020) 223–237, <https://doi.org/10.1038/s41575-019-0258-z>.
- [9] X. Huang, S. Nie, M. Xie, Interaction between gut immunity and polysaccharides, *Crit. Rev. Food Sci. Nutr.* 57 (14) (2017) 2943–2955, <https://doi.org/10.1080/10408398.2015.1079165>.
- [10] W. Yang, P. Zhao, X. Li, L. Guo, W. Gao, The potential roles of natural plant polysaccharides in inflammatory bowel disease: a review, *Carbohydr. Polym.* 277 (2022), 118821, <https://doi.org/10.1016/j.carbpol.2021.118821>.
- [11] W. Niu, X. Chen, R. Xu, H. Dong, F. Yang, Y. Wang, Z. Zhang, J. Ju, Polysaccharides from natural resources exhibit great potential in the treatment of ulcerative colitis: a review, *Carbohydr. Polym.* 254 (2021), 117189, <https://doi.org/10.1016/j.carbpol.2020.117189>.
- [12] C. Tang, R. Ding, J. Sun, J. Liu, J. Kan, C. Jin, The impacts of natural polysaccharides on intestinal microbiota and immune responses - a review, *Food Funct.* 10 (2019) 2290, <https://doi.org/10.1039/c8fo01946k>.
- [13] R.E. Chambers, J.R. Clamp, An assessment of methanolysis and other factors used in the analysis of carbohydrate-containing materials, *Biochem. J.* 125 (1971) 1009–1018, <https://doi.org/10.1042/bj1251009>.
- [14] A.A.T. Nyman, F.L. Aachmann, F. Rise, S. Ballance, A.B.C. Samuelsen, Structural characterization of a branched (1 → 6)- $\alpha$ -mannan and  $\beta$ -glucans isolated from the fruiting bodies of *Cantharellus cibarius*, *Carbohydr. Polym.* 146 (2016) 197–207, <https://doi.org/10.1016/j.carbpol.2016.03.052>.
- [15] V.L. Singleton, J.A. Rossi, Colorimetry of total phenolics with phosphomolybdic-phosphotungstic acid reagent, *Am. J. Enol. Viticult.* 16 (1965) 144–158. (<https://www.ajevonline.org/content/16/3/144>).
- [16] M.M. Bradford, A rapid and sensitive method for the quantitation of microgram quantities of protein utilizing the principle of protein-dye binding, *Anal. Chem.* 72 (1–2) (1976) 248–254, [https://doi.org/10.1016/0003-2697\(76\)90527-3](https://doi.org/10.1016/0003-2697(76)90527-3).
- [17] S. Wirtz, V. Popp, M. Kindermann, K. Gerlach, B. Weigmann, S. Fichtner-Feigl, M. F. Neurath, Chemically induced mouse models of acute and chronic intestinal inflammation, *Nat. Protoc.* 12 (7) (2017) 1295–1309, <https://doi.org/10.1038/nprot.2017.044>.
- [18] H. Sann, J. Erichsen, M. Hessmann, A. Pahl, A. Hoffmeyer, Efficacy of drugs used in the treatment of IBD and combinations thereof in acute DSS-induced colitis in mice, *Life Sci.* 92 (12) (2013) 708–718, <https://doi.org/10.1016/j.lfs.2013.01.028>.
- [19] Y.-P. Fu, B. Feng, Z.-K. Zhu, X. Feng, S.-F. Chen, L.-X. Li, Z.-Q. Yin, C. Huang, X.-F. Chen, B.-Z. Zhang, R.-Y. Jia, X. Song, C. Lv, G.-Z. Yue, G. Ye, X.-X. Liang, C.-L. He, L.-Z. Yin, Y.-F. Zou, The polysaccharides from *Codonopsis pilosula* modulates the immunity and intestinal microbiota of cyclophosphamide-treated immunosuppressed mice, *Molecules* 23 (2018) 1801, <https://doi.org/10.3390/molecules23071801>.

- [20] Y. Chengxiao, W. Dongmei, Z. Kai, L. Hou, H. Xiao, T. Ding, D. Liu, X. Ye, R. J. Linhardt, S. Chen, Challenges of pectic polysaccharides as a prebiotic from the perspective of fermentation characteristics and anti-colitis activity, *Carbohydr. Polym.* 270 (2021), 118377, <https://doi.org/10.1016/j.carbpol.2021.118377>.
- [21] B. Chassaing, J.D. Aitken, M. Malleshappa, M. Vijay-Kumar, Dextran sulfate sodium (DSS)-induced colitis in mice, *Curr. Protoc. Immunol.* 104 (2014) 15.25.1–15.25.14, <https://doi.org/10.1002/0471142735.im1525s104>.
- [22] Y. Aratani, Myeloperoxidase: Its role for host defense, inflammation, and neutrophil function, *Arch. Biochem. Biophys.* 640 (2018) 47–52, <https://doi.org/10.1016/j.abb.2018.01.004>.
- [23] W. Yang, D. Ren, Y. Zhao, L. Liu, X. Yang, Fuzhuan brick tea polysaccharide improved ulcerative colitis in association with gut microbiota-derived tryptophan metabolism, *J. Agric. Food Chem.* 69 (2021) 8448–8459, <https://doi.org/10.1021/acs.jafc.1c02774>.
- [24] C. Sabater, J.A. Molina-Tijeras, T. Vezza, N. Corzo, A. Montilla, P. Utrillab, Intestinal anti-inflammatory effects of artichoke pectin and modified pectin fractions in the dextran sulfate sodium model of mice colitis. Artificial neural network modelling of inflammatory markers, *Food Funct.* 10 (2019) 7793–7805, <https://doi.org/10.1039/c9fo02221j>.
- [25] M. Jin, Y. Wang, X. Yang, H. Yin, S. Nie, X. Wu, Structure characterization of a polysaccharide extracted from noni (*Morinda citrifolia* L.) and its protective effect against DSS-induced bowel disease in mice, *Food Hydrocolloid.* 90 (2019) 189–197, <https://doi.org/10.1016/j.foodhyd.2018.11.049>.
- [26] M.S. Elshahed, A. Miron, A.C. Aprotosoia, M.A. Farag, Pectin in diet: interactions with the human microbiome, role in gut homeostasis, and nutrient-drug interactions, *Carbohydr. Polym.* 255 (2021), 117388, <https://doi.org/10.1016/j.carbpol.2020.117388>.
- [27] Q. Song, Y. Wang, L. Huang, M. Shen, Y. Yu, Q. Yu, Y. Chen, J. Xie, Review of the relationships among polysaccharides, gut microbiota, and human health, *Food Res. Int.* 140 (2021), 109858, <https://doi.org/10.1016/j.foodres.2020.109858>.
- [28] A.-M. Davila, Fo Blachier, M. Gotteland, M. Andriamihaja, P.-H. Benetti, Y. Sanz, D. Toméa, Intestinal luminal nitrogen metabolism: role of the gut microbiota and consequences for the host, *Pharmacol. Res.* 68 (2013) 95–107, <https://doi.org/10.1016/j.phrs.2012.11.005>.
- [29] F. Blachier, F. Mariotti, J.F. Huneau, D. Tomé, Effects of amino acid-derived luminal metabolites on the colonic epithelium and physiopathological consequences, *Amino Acids* 33 (2007) 547–562, <https://doi.org/10.1007/s00726-006-0477-9>.
- [30] A. Stinccone, A. Prigione, T. Cramer, M.M.C. Wamelink, K. Campbell, E. Cheung, V. Olin-Sandoval, N.-M. Gruning, A. Krüger, M.T. Alam, M.A. Keller, M. Breitenbach, K.M. Brindle, J.D. Rabinowitz, M. Ralsler, The return of metabolism: biochemistry and physiology of the pentose phosphate pathway, *Biol. Rev.* 90 (2015) 927–963, <https://doi.org/10.1111/brv.12140>.
- [31] W. Zhang, H. Cheng, Y. Gui, Q. Zhan, S. Li, W. Qiao, A. Tong, Mannose treatment: a promising novel strategy to suppress inflammation, *Front. Immunol.* 12 (2021), 756920, <https://doi.org/10.3389/fimmu.2021.756920>.
- [32] D.-S. Lee, E.-S. Lee, M.M. Alam, J.-H. Jang, H.-S. Lee, H. Oh, Y.-C. Kim, S. Manzoor, Y.-S. Koh, D.-G. Kang, D.H. Lee, Soluble DPP-4 up-regulates toll-like receptors and augments inflammatory reactions, which are ameliorated by vildagliptin or mannose-6-phosphate, *Metabolism* 65 (2016) 89–101, <https://doi.org/10.1016/j.metabol.2015.10.002>.
- [33] A. Leuti, Domenico Fazio, M. Fava, A. Piccoli, S. Oddi, M. Maccarrone, Bioactive lipids, inflammation and chronic diseases, *Adv. Drug Deliv. Rev.* 159 (2020) 133–169, <https://doi.org/10.1016/j.addr.2020.06.028>.
- [34] Z. Yuan, L. Yang, X. Zhang, P. Ji, Y. Hua, Y. Wei, Mechanism of Huang-lian-Jie-du decoction and its effective fraction in alleviating acute ulcerative colitis in mice: regulating arachidonic acid metabolism and glycerophospholipid metabolism, *J. Ethnopharmacol.* 259 (2020), 112872, <https://doi.org/10.1016/j.jep.2020.112872>.
- [35] Q. Tang, S. Cang, J. Jiao, W. Rong, H. Xu, K. Bi, Q. Li, R. Liu, Integrated study of metabolomics and gut metabolic activity from ulcerative colitis to colorectal cancer: the combined action of disordered gut microbiota and linoleic acid metabolic pathway might fuel cancer, *J. Chromatogr. A* 1629 (2020), 461503, <https://doi.org/10.1016/j.chroma.2020.461503>.
- [36] S. Tian, J. Li, R. Li, Z. Liu, W. Dong, Decreased serum bilirubin levels and increased uric acid levels are associated with ulcerative colitis, *Med. Sci. Monit.* 24 (2018) 6298–6304, <https://doi.org/10.12659/MSM.909692>.
- [37] F. Zhu, D. Feng, T. Zhang, L. Gu, W. Zhu, Z. Guo, Y. Li, N. Lu, J. Gong, N. Li, Altered uric acid metabolism in isolated colonic Crohn's disease but not ulcerative colitis, *J. Gastroenterol. Hepatol.* 34 (1) (2019) 154–161, <https://doi.org/10.1111/jgh.14356>.
- [38] S.H. Kim, W. Lee, D. Kwon, S. Lee, S.W. Son, M.-S. Seo, K.S. Kim, Y.-H. Lee, S. Kim, Y.-S. Jung, Metabolomic analysis of the liver of a dextran sodium sulfate-induced acute colitis mouse model: implications of the gut–liver connection, *Cells* 9 (2020) 341, <https://doi.org/10.3390/cells9020341>.
- [39] T. Ohkusa, S. Koido, Intestinal microbiota and ulcerative colitis, *J. Infect. Chemother.* 21 (11) (2015) 761–768, <https://doi.org/10.1016/j.jiac.2015.07.010>.
- [40] Z. Wu, S. Huang, T. Li, N. Li, D. Han, B. Zhang, Z.Z. Xu, S. Zhang, J. Pang, S. Wang, G. Zhang, J. Zhao, J. Wang, Gut microbiota from green tea polyphenol-dosed mice improves intestinal epithelial homeostasis and ameliorates experimental colitis, *Microbiome* 9 (2021) 184, <https://doi.org/10.1186/s40168-021-01115-9>.
- [41] A. Rodríguez-Nogales, F. Algieri, J. Garrido-Mesa, T. Vezza, M.P. Utrilla, N. Chuec, F. García, M.E. Rodríguez-Cabezas, J. Gálvez, Intestinal anti-inflammatory effect of the probiotic *Saccharomyces boulardii* in DSS induced colitis in mice: Impact on microRNAs expression and gut microbiota composition, *J. Nutr. Biochem.* 61 (2018) 129–139, <https://doi.org/10.1016/j.jnutbio.2018.08.005>.
- [42] C. Wang, J. Zhao, H. Zhang, Y.K. Lee, Q. Zhai, W. Chen, Roles of intestinal bacteroides in human health and diseases, *Crit. Rev. Food Sci. Nutr.* 61 (21) (2021) 3518–3536, <https://doi.org/10.1080/10408398.2020.1802695>.
- [43] R. Dziarski, S.Y. Park, D.R. Kashyap, S.E. Dowd, D. Gupta, Pglyrp-regulated gut microflora *Prevotella falsenii*, *Parabacteroides distans* and *Bacteroides eggerthii* enhance and *Alistipes finegoldii* attenuates colitis in mice, *PLoS One* 11 (1) (2016), e0146162, <https://doi.org/10.1371/journal.pone.0146162>.
- [44] F. Wan, H. Han, R. Zhong, M. Wang, S. Tang, S. Zhang, F. Hou, B. Yi, H. Zhang, Dihydroquercetin supplement alleviates colonic inflammation potentially through improved gut microbiota community in mice, *Food Funct.* 12 (22) (2021) 11420–11434, <https://doi.org/10.1039/d1fo01422f>.
- [45] M. Yang, C. Yang, Y. Zhang, X. Yan, Y. Ma, Y. Zhang, Y. Cao, Q. Xu, K. Tu, M. Zhang, An oral pH-activated "nano-bomb" carrier combined with berberine by regulating gene silencing and gut microbiota for site-specific treatment of ulcerative colitis, *Biomater. Sci.* 10 (4) (2022) 1053–1067, <https://doi.org/10.1039/d1bm01765a>.
- [46] B.J. Parker, P.A. Wearsch, A.C.M. Veloo, A. Rodríguez-Palacios, The genus *Alistipes*: gut bacteria with emerging implications to inflammation, cancer, and mental health, *Front. Immunol.* 11 (2020) 906, <https://doi.org/10.3389/fimmu.2020.00906>.
- [47] M. Borges-Canha, J.P. Portela-Cidade, M. Dinis-Ribeiro, A.F. Leite-Moreira, P. Pimentel-Nunes, Role of colonic microbiota in colorectal carcinogenesis: a systematic review, *Rev. Esp. De Enferm. Dig.* 107 (2015) 659–671, <https://doi.org/10.17235/reed.2015.3830/2015>.
- [48] P. Li, N. Xiao, L. Zeng, J. Xiao, J. Huang, Y. Xu, Y. Chen, Y. Ren, B. Du, Structural characteristics of a mannoglucan isolated from Chinese yam and its treatment effects against gut microbiota dysbiosis and DSS-induced colitis in mice, *Carbohydr. Polym.* 250 (2020), 116958, <https://doi.org/10.1016/j.carbpol.2020.116958>.
- [49] N. Larsen, C. Bussolo de Souza, L. Krych, T. Barbosa Cahu, M. Wiese, W. Kot, K. M. Hansen, A. Blennow, K. Venema, L. Jaspersen, Potential of pectins to beneficially modulate the gut microbiota depends on their structural properties, *Front. Microbiol.* 10 (2019) 223, <https://doi.org/10.3389/fmicb.2019.00223>.
- [50] S.J. Bang, G. Kim, M.Y. Lim, E.J. Song, D.H. Jung, J.S. Kum, Y.D. Nam, C.S. Park, D. H. Seo, The influence of in vitro pectin fermentation on the human fecal microbiome, *AMB Express* 8 (1) (2018) 98, <https://doi.org/10.1186/s13568-018-0629-9>.
- [51] Q. Nie, J. Hu, H. Gao, M. Li, Y. Sun, H. Chen, S. Zuo, Q. Fang, X. Huang, J. Yin, S. Nie, Bioactive dietary fibers selectively promote gut microbiota to exert anti-diabetic effects, *J. Agric. Food Chem.* 69 (25) (2021) 7000–7015, <https://doi.org/10.1021/acs.jafc.1c01465>.
- [52] J. Zou, C. Liu, S. Jiang, D. Qian, J. Duan, Cross talk between gut microbiota and intestinal mucosal immunity in the development of ulcerative colitis, *Infect. Immun.* 89 (2021) e00014–e00021, <https://doi.org/10.1128/IAI.00014-21>.
- [53] Y. Chang, L. Zhai, J. Peng, H. Wu, Z. Bian, H. Xiao, Phytochemicals as regulators of Th17/Treg balance in inflammatory bowel diseases, *Biomed. Pharmacother.* 141 (2021), 111931, <https://doi.org/10.1016/j.biopha.2021.111931>.